

Transmission of Gravity Waves and Planetary Waves in the Middle Atmosphere Based on Lidar and Rocket Measurements

C.R. Philbrick and B. Chen

Communications and Space Sciences Laboratory, Penn State University, University Park, PA 16802, U.S.A.

ABSTRACT

Using a set of results obtained from LIDAR measurements during February to April 1986 at Poker Flat Research Range, Alaska, an investigation of the planetary and gravity waves in the middle atmosphere has been made. The measurement period included a moderate stratospheric warming which reached its peak response at 65°N latitude on 20/21 February. The wave activity was modulated greatly in amplitude during the stratospheric warming. The modeled periods, amplitudes and phases of the two primary wave components agree well with the planetary wave numbers 1 and 2. The peak of the planetary wave amplitude appears to be due to the sum effects of the constructive interference of the waves. The peak of the amplitude of the planetary waves on 21 February corresponds to a major increase in profile structure and results in a stratosphere density gradient that is convectively unstable over a thick layer.

INTRODUCTION

The structure profiles in the middle atmosphere are known to be frequently and considerably disturbed in the northern winter /1/. LIDAR sounding from the ground offers the new possibility of studying the characteristics of wave propagation in the profiles of density and temperature for examining the consequences of the dynamical processes in the middle atmosphere.

From February 14 to March 9, 1986, the density perturbations in the high latitude middle atmosphere were measured continuously by a lidar /2,3/ at Poker Flat Research Range near Fairbanks, Alaska. During the measurement period, rocket measurements were made on a few dates in order to compare the results with those obtained by the lidar.

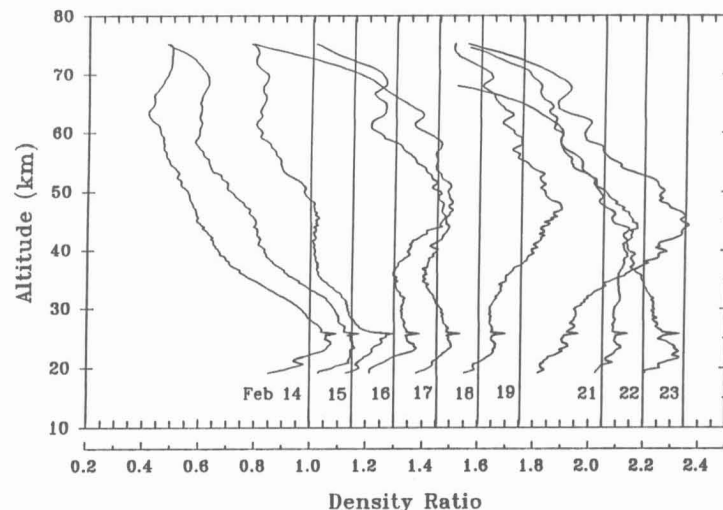


Fig. 1. Density ratio as a function of date for 10 days leading into stratospheric warming. Below 25 km the profile is modified by particle scatter and shutter function.

The full night mean density profiles are shown in Figure 1 and mean temperature profiles are shown in Figure 2. Clearly, there was a large perturbation of density at the altitude of 40-50 km which reaches a maximum on 21 February. This perturbation corresponds to a period of a moderate stratospheric warming and appears to correlate with the constructive interference, or the superposition of planetary waves. It corresponds, as well, to a period of extreme wave activity in the stratosphere and the relative reduction of gravity wave activity in the mesosphere. Because of the hydrostatic response of the atmosphere, the maximum in the temperature perturbation is observed to occur about two density scale heights (about 15 km) below the density perturbation.

Naujokat and Labitzke /4/ have reported the stratospheric warming about the same time and latitude based on the satellite data. The dynamical behavior of the middle atmosphere during a stratospheric warming was studied by various authors, for instance, Offermann and Gerndt, /5/, McIntyre and Palmer, /6/, Haynes and McIntyre, /7/, Holton, /8/, Salby, /9/, etc. In this paper, we place emphasis on the characteristics of the planetary waves and gravity waves during a stratospheric warming. First, a model of planetary waves was developed to describe the periods and phases of the principle wave components. A spectral analysis was then applied to the short period signal, which are normally associated with the gravity waves. The analysis shows extraordinarily strong activity of the short period waves was present in the stratosphere on the date when the warming occurred.

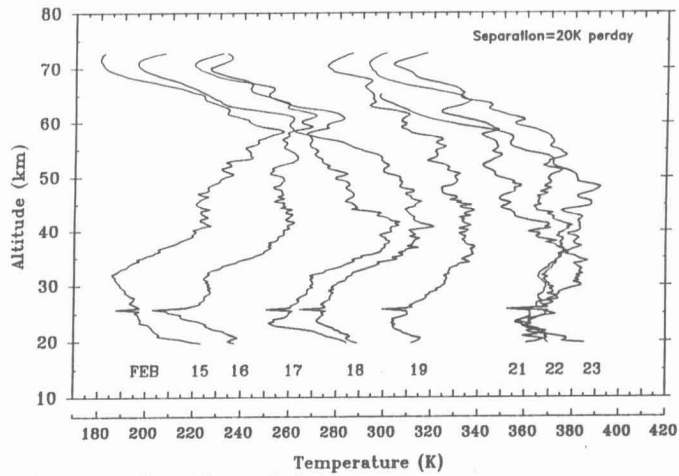


Fig. 2. Temperature as a function of date.

#### CHARACTERISTICS OF THE PLANETARY WAVES

To find the periods and phases of the planetary waves, a one dimensional model is developed to simulate the variations of the density between February 15 and March 9, 1986.

The model has the following form:

$$D(x, t) = \text{Re}[\sum_i A_i e^{j(\omega_i t - kx)}] = \text{Re}[\sum_i (a_i + jb_i) e^{j(\omega_i t - kx)}]$$

where  $D$  is the density ratio,  $x$  is the space coordinate,  $t$  is the time parameter,  $A_i = a_i + jb_i$  is the complex amplitude and  $k$  is the wavenumber in  $x$  direction.

Since the measurement was done at a fixed place,  $x$  can be set to be zero in the model. Now that only the time development of the wave needs to be simulated, the parameters to be estimated are as following:

$$\begin{aligned} \omega_i &: \text{wavefrequency;} \\ (a_i^2 + b_i^2)^{\frac{1}{2}} &: \text{waveamplitude;} \\ \arctan\left(\frac{b_i}{a_i}\right) &: \text{wavephase} \end{aligned}$$

The frequencies of the planetary waves were determined by spectral estimation. Since there were only 22 full-night mean densities available, an accurate estimation was difficult to compute. Thus both parametric estimations (Maximum Entropy) and non-parametric estimation (Blackman-Tukey) were performed and the results were compared. For convenience, the densities had been converted to density ratios by using the annual mean in U.S. Standard Atmosphere (1976) as the basis. The mean of the density ratios at each altitude (5-km steps, from 25 km to 65 km) had been subtracted so that the expectations of the signals became zeros. Figure 3 shows the power spectra at different altitudes from 25 km to 65 km by Maximum Entropy method. It is interesting to find that there were several dominant frequencies, for instance,  $f_1=0.07$ ,  $f_2=0.1$ ,  $f_3=0.225$  and  $f_4=0.33$ . Thus the frequencies,  $\omega_i$ , in the model can be determined. The number of the frequencies selected also implies the number of sinusoids embedded in the density signal.

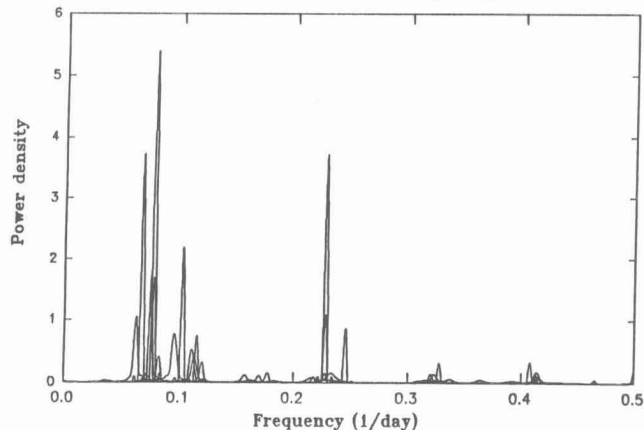


Fig. 3. Spectral estimation of the density signals at different altitudes (25-65 km) by Maximum Entropy method.

A computer program was developed to perform the nonlinear fitting. With frequencies being fixed, amplitudes and phases of the four waves were represented by a parameter array  $B$ . A merit function was defined which depended on the given density data as well as the parameter array  $B$ . The array  $B$  was updated by the minimization of the merit function. Since the model was dependent nonlinearly on the parameters, the minimization was carried out iteratively after trial values were given.

Solid line: Modeled; Symbol: Measured

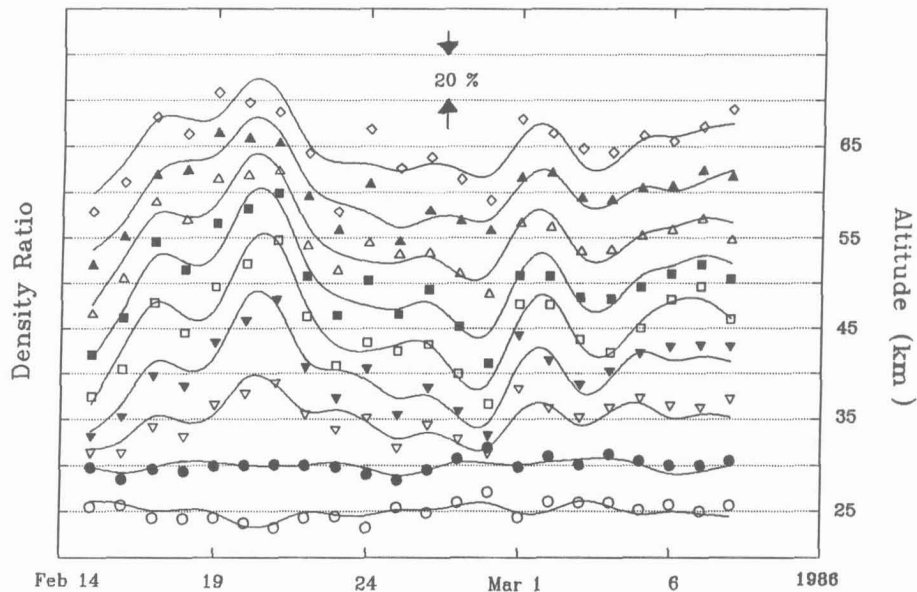


Fig. 4. Agreement between modeled and measured density waves.

The results of the simulation are shown in Figure 4, which also presents the agreement of the modeled density variations and the measured ones. The satisfactory agreement in turn gives creditability to the Maximum Entropy method in power spectrum estimation. If a horizontal velocity of 10 m/s is assumed as typical of synoptic scales, the first two sinusoids correspond to planetary wave 1 and 2.

#### CHARACTERISTICS OF THE GRAVITY WAVES

To see the wave lengths as well as the activity of the gravity waves during the stratospheric warming, the power spectra of the gravity waves at different altitudes from February 18 to March 9 were estimated (the moderate stratospheric warming occurred around February 21). First, we assume that the small perturbations in densities were solely caused by gravity waves. Then a polynomial of degree 5 obtained by LSE method was used to simulate each of the 5-minute density profiles. The difference of the density profile and its LSE simulation was assumed to be the signal of the gravity waves.

The results of the spectral estimation at different altitude ranges are shown in Figure 5. The typical wave length was 15 km. The stratospheric warming periods were Feb.20-21 and Mar.6 through the end of the month (available in the winter report of Naujokat and Labitzke /4/).

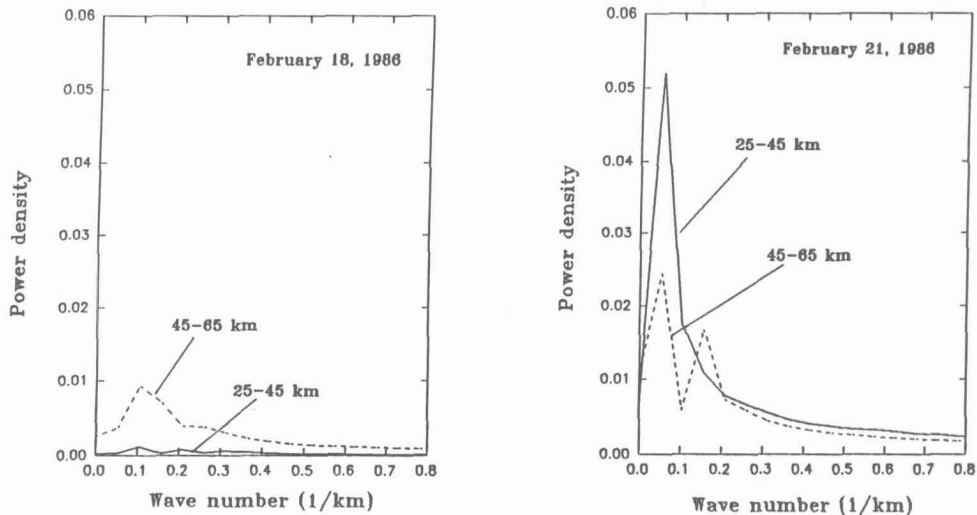


Fig. 5. Gravity wave spectra on February 18 and 21 showing the increase in intensity of the wave activity at the peak of the warming.

Figure 5 presents the comparison of the gravity wave spectra at different altitude ranges on the dates around the moderate stratospheric warming. A stronger wave activity was seen at 25-45 km than that at 45-65 km on Feb. 21 and during a recorded major warming from March 6 to the end of the month, while on the other days the spectra showed just the opposite.

Since the amplitudes of gravity waves tend to grow while the waves are propagating upward, we expected to see relatively greater power spectra at 45-65 km range than that at 25-45 km. However, Fig 4 shows the contrary. The reduction in the relative amplitude of gravity wave activity at 45-65 km during the warmings could be explained in the constructive interference of the planetary waves reducing the stability of the surrounding atmosphere so that the level of significant wave breaking was substantially lowered. Such phenomenon had been discussed by Lindzen /10/ and Fritts /11/.

## CONCLUSION

Middle atmosphere densities measured by a Rayleigh scatter LIDAR during February and March 1986 showed strong wave-like perturbations. The extended and high resolution sequences of the continuous measurements provided a solid base for the simulation of the long period variations as well as the investigation of the gravity wave activity.

The wave-like variations of the density were modeled satisfactorily with a superposition of several sinusoids. Periods of the sinusoids were found to be 14, 10, 4 and 3 days by spectrum analysis at the fixed altitudes. Parametric estimation (like MEM) is attractive with short data records.

The spatial spectrum analysis of the gravity waves showed strong gravity wave activity at 25-45 km during stratospheric warming. The lack of gravity wave activity at 45-65 km implied that the level of significant wave breaking was lowered below 50 km during the event. This could be explained due to the constructive interference of the planetary waves which modulated the stability of the surrounding atmosphere.

While the source for the stratospheric warming must be from the large energy source of the planetary waves, the mechanism for the event may be a large scale upset of atmospheric stability. It may be that the constructive interference of the planetary waves result in such large density perturbations that the static stability of the stratosphere is upset. In fact, planetary wave breaking could be the physical process that leads to the large amount of small scale wave structure observed near the peak of the event (the large vorticity increase). The planetary wave breaking would generate a range of scales of shorter waves and vortices as the atmosphere re-establishes equilibrium, and in addition the continuous phase shift between the principle components would also contribute to the rapidity of the return to normal winter conditions. The observed temperature increase, for which these events are named, may be just the normal response of the adiabatic heating due to the higher density at about two scale heights above, caused by the constructive interference of the waves.

*Acknowledgements.* Discussions with several colleagues, particularly D. Offermann, U. Von Zahn, M. E. McIntyre, J. D. Mathews, E. V. Thrane and D. G. Fritts, are gratefully acknowledged. Thanks are also due to K. Bounar for his initial work on the data set and D. Sipler in obtaining the data set.

## REFERENCES

1. C.R. Philbrick, F.J. Schmidlin, K.U. Grossmann, G. Lange, D. Offermann, K.D. Baker, D. Krankowsky and U. von Zahn, Density and temperature structure over northern Europe, *J. Atmos. Terr. Phys.* 47, 159-172 (1985).
2. C.R. Philbrick, D.P. Sipler, B.E. Dix, G. Davidson, W.P. Moskowitz, C. Trowbridge, R. Sluder, F.J. Schmidlin, L.D. Mendenhall, K.H. Bhavnani and K.J. Hahn, Measurements of the high latitude middle atmosphere properties using LIDAR, *AFGL-TR-87-0053* (1987).
3. C.R. Philbrick, D.P. Sipler, G. Davidson and W.P. Moskowitz, Remote sensing of structure properties in the middle atmosphere using LIDAR, *Proceedings of OSA Meeting on Laser and Optical Remote Sensing*, 120-123 (1987).
4. B. Naujokat and K. Labitzke, Beilage zur berliner wetterkarte. *Climate Analysis CTR.* (1986).
5. D. Offermann, R. Gerndt, R. Kuchler, K. Baker, W.R. Pendleton, W. Mayer, U. Von Zahn, C.R. Philbrick and F.J. Schmidlin, Mean state and Long term variations in the winter atmosphere above northern Scandinavia. *J. Atmos. & Terr. Phys.* 49, 655-674 (1987).
6. M.E. McIntyre and T.N. Palmer, Breaking Planetary Waves in the Stratosphere, *Nature* 305, 593-600 (1983).
7. P.H. Haynes and M.E. McIntyre, On the representation of Rossby-wave critical layers and wave breaking in zonally truncated models, *J. Atmos. Sci.* 44, 2359-2382 (1986).
8. J.R. Holton, The influence of gravity wave breaking on the general circulation of the middle atmosphere, *J. Atmos. Sci.* 39, 791-799 (1982).
9. M.L. Salby, Survey of planetary-scale travelling waves: The state of theory and observations. *Revs. Geophys. Space Phys.* 22, 209-236 (1984).
10. R.S. Lindzen, Turbulence and stress owing to gravity wave and tidal breakdown, *J. Geophys. Res.* 86, 9707-9714 (1981).
11. D.C. Fritts, Gravity waves saturation in the middle atmosphere: A review of theory and observation. *Rev. Geophys.* 22, 275-307 (1984).